**Supplementary information**

**Exciplex Emissions Derived from Exceptionally Long-Distanced Donor and Acceptor Molecules**

Yong-Jin Pu*[1, 2], Yuki Koyama[1, 2], Daisuke Otsuki[2], Minjun Kim[1], Hiroya Chubachi[2], Yuki Seino[1], Kazushi Enomoto[1], Naoya Aizawa[1, 3]

[1]RIKEN Center for Emergent Matter Science (CEMS) , Wako, Saitama 351-0198, Japan.

[2]Graduate School of Organic Materials Science, Yamagata University, Yonezawa, Yamagata 992-8510 Japan.

[3]JST-PRESTO, Kawaguchi, Saitama 332-0012, Japan.

*E-mail: yongjin.pu@riken.jp

**Materials.** TAPC and CBP were purchased from e-Ray. MTDATA, B3PyPB, and B4PyMPm were purchased from Lumtec. NPD, TCTA, and DNTPD were purchased from Chemipro Kasei. PMA was purchased from Aldrich. PEDOT:PSS was purchased from Clevious. DMA and DCA was synthesized by general Suzuki coupling methods.

**Measurements of physical properties.** UV-vis absorption spectra were recorded on a Shimadzu UV-3150 spectrometer. The HOMO levels were measured by photoelectron yield spectroscopy, and the LUMO levels were estimated from the HOMO levels and the optical energy gaps determined from the absorption spectra. PL spectra were measured using a Horiba Fluoromax-4 fluorometer. PL decay curves were measured using a Horiba Fluorolog–3. Fluorescence lifetimes were extracted from the transient PL decay curves by performing two- or three-exponential decay fitting and deconvolution with the instrument response function $IRF(t)$. The fitting function is expressed as the equation S1:

$$I(t) = IRF(t) \otimes \sum_{i=1}^{n} A_i \exp\left(-\frac{t}{\tau_i}\right)$$

(S1)

where $I(t)$ is the PL intensity, $A_i$ is the exponential pre-factor of each exponential decay component, and $\tau_i$ is the fluorescence lifetime of each exponential decay component, $n$ is the number of exponential decay components. The time-integrated fluorescence intensity of each exponential decay component $I_{i,\text{int}}(t)$ is

$$I_{i,\text{int}}(t) = \int_0^\infty A_i \exp\left(-\frac{t}{\tau_i}\right) dt = A_i \tau_i \qquad \text{(S2)}$$

The relative time-integrated fluorescence intensity of each exponential decay component to the sum of the intensity for all components $\Phi_i$ is

$$\Phi_i = \frac{I_{i,\text{int}}(t)}{\sum_{i=1}^{n} I_{i,\text{int}}(t)} = \frac{A_i \tau_i}{\sum_{i=1}^{n} A_i \tau_i} \qquad \text{(S3)}$$

The intensity-weighted average fluorescence lifetime $\langle \tau \rangle$ is

$$\langle \tau \rangle = \frac{\sum_{i=1}^{n} \tau_i I_{i,\text{int}}(t)}{\sum_{i=1}^{n} I_{i,\text{int}}(t)} = \frac{\sum_{i=1}^{n} A_i \tau_i^2}{\sum_{i=1}^{n} A_i \tau_i} \qquad \text{(S4)}$$

**Device fabrication and characterization.** All devices were grown on glass substrates pre-coated with a 130 nm thick layer of indium tin oxide (ITO) with a sheet resistance of 15 Ω/square. The substrates were cleaned with ultra-purified water and organic solvents and then by exposure to a UV-ozone atmosphere. The organic compounds were successively deposited onto the ITO substrate under vacuum (~$10^{-5}$ Pa). LiF and Al were patterned using a shadow mask with an array of openings (2 mm × 2 mm) without breaking the vacuum. All devices were encapsulated under a nitrogen atmosphere immediately after preparation using epoxy glue and glass lids. EL spectra were collected using an optical multichannel analyser (Hamamatsu Photonics PMA-12). The current density-voltage and luminance-voltage characteristics were measured using a Keithley 2400 source measurement unit and a Minolta CS200 luminance-meter respectively. The transient EL decay was measured using a function generator (33220A, Agilent), an oscilloscope (DPO 3052, Tektronix), and a Si photodetector (H7826, Hamamatsu Photonics).

**Synthesis**

General reagent information: 2-(3,5-Dimethoxyphenyl)-4,4,5,5-tetramethyl-1,3,2-dioxaborolan, 9,10-dibromoanthracene, tetrakis(triphenylphosphine)palladium(0), 9,10-bis(4,4,5,5,-tetramethyl-1,3,2-diocaborolan-2-yl)anthracene were purchased from TCI. Potassium carbonate, toluene, ethanol, anhydrous MgSO$_4$ were purchased from Kanto Chemical. Tris(dibenzylideneacetone)dipalladium(0), and 2-dicyclohexylphosphino-2',6'-dimethoxybiphenyl were purchased from Aldrich. 5-Bromo-1,3-benzenedicarbonitrile (>98%) was purchased from BOC Sciences. All reagents and solvents were used as received without further purification.

General analytical information: All compounds were characterized by ^{1}H-NMR, ^{13}C-NMR, matrix-assisted laser desorption/ionization time of flight (MALDI-TOF) mass spectrometry (MS) and elemental analysis. ^{1}H- and ^{13}C-NMR spectra were recorded on JASTEC JNM-AL400 (400 MHz) spectrometer. Chemical shifts are given in ppm relative chloroform. Mass spectrum was performed on a Bruker Daltonics Ultraflex spectrometer by using dithranol as the matrix.

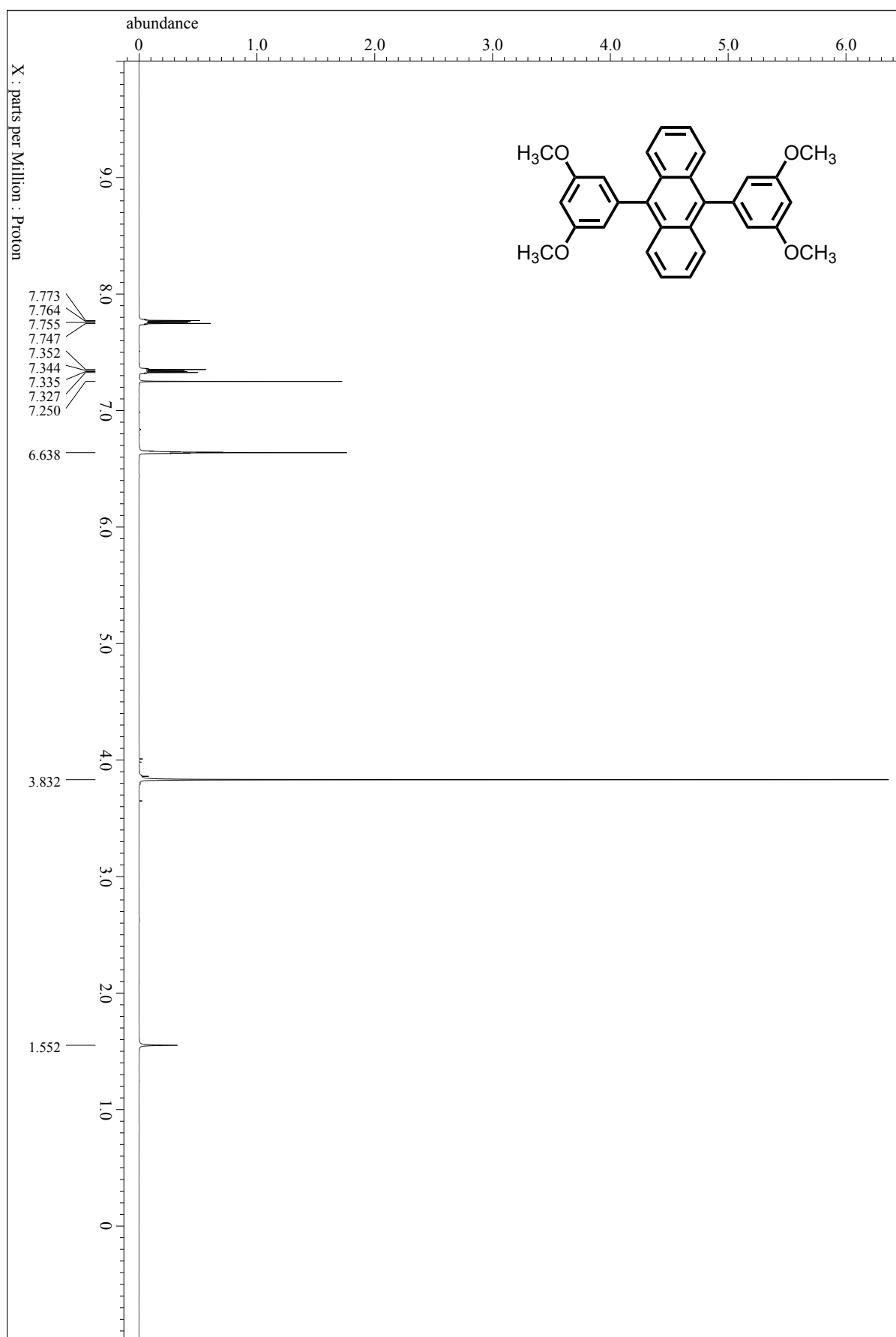9,10-Bis(3,5-dimethoxyphenyl)anthracene (DMA)
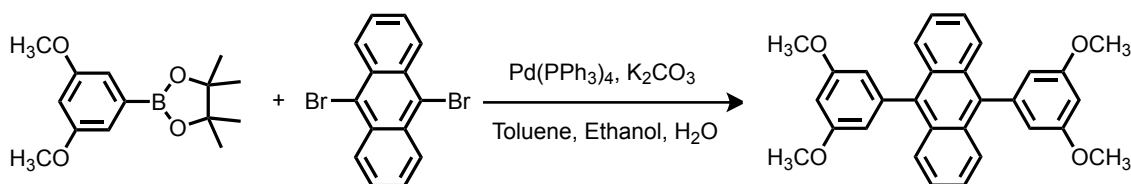


2-(3,5-Dimethoxyphenyl)-4,4,5,5-tetramethyl-1,3,2-dioxaborolane (2.36 g, 8.93 mmol), 9,10-dibromoanthracene (1.20 g, 3.57 mmol), potassium carbonate (1.23 g, 8.93 mmol), toluene (60 mL), ethanol (30 mL) and water (30 mL) were added to a three-neck flask, and nitrogen passed through the mixture for 1 h. Then, tetrakis(triphenylphosphine)palladium(0) (0.120 g, 0.110 mmol) was added and the resulting mixture was vigorously stirred for 24 hours at reflux temperature under nitrogen. The resulting mixture was cooled to room temperature. Then, water was added to the mixture, and the organic layer was extracted with toluene, washed with water. The organic layer was separated, dried over anhydrous $MgSO_4$, and evaporated. The small amount of solution was purified by silica gel flash chromatography (EtOAc/hexane = 1:5 v/v). Then, recrystallization was performed by toluene and ethanol to afford DMA as an off-white solid (1.66 g, 86%): ^{1}H-NMR (400 MHz, $CDCl_3$): δ 7.7 5 (dd, 4H, $J$ = 6.8 Hz, $J$ = 3.6 Hz), 7.34 (dd, 4H, $J$ = 6.8 Hz, $J$ = 3.2 Hz), 6.67–6.61 (m, 6H), 3.83 (s, 12H) ppm. ^{13}C-NMR (100 MHz, $CDCl_3$): δ 161.1, 141.2, 137.7, 129.8, 127.1, 125.6, 109.0, 100.1, 55.6. MS (MALDI-TOF, $m/z$): Calcd for $C_{30}H_{26}O_4$: 450.18; found: 450.10. Elemental Anal.: Calcd for $C_{30}H_{26}O_4$: C 79.98, H 5.82; found: C 80.12, H 5.72.

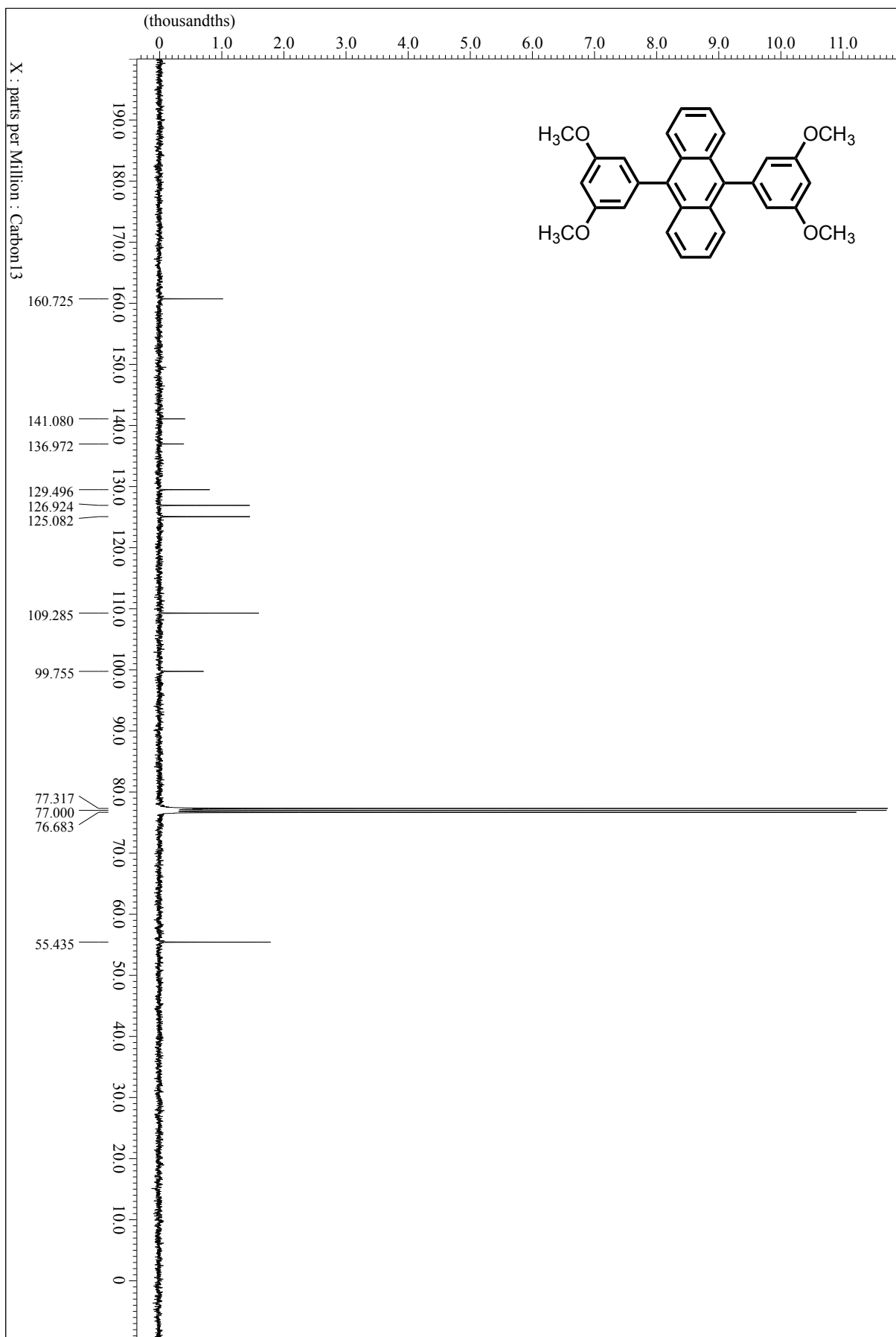9,10-Bis(3,5-dicyanophenyl)anthracene (DCA)
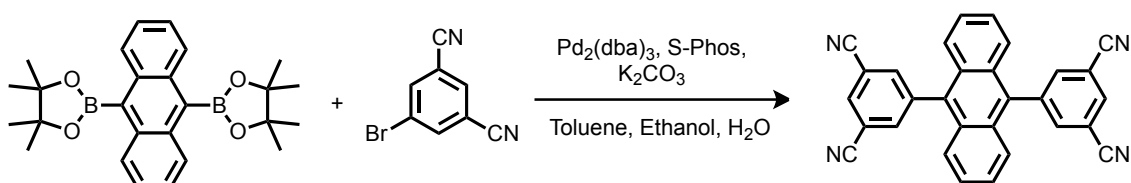


9,10-Bis(4,4,5,5,-tetramethyl-1,3,2-diocaborolan-2-yl)anthracene (1.00 g, 2.32 mmol), 5-bromo-1,3-benzenedicarbonitrile (1.44 g, 6.96 mmol), potassium carbonate (0.962 mg, 6.96 mmol), toluene (50 mL), ethanol (25 mL) and water (25 mL) were added to a three-neck flask, and
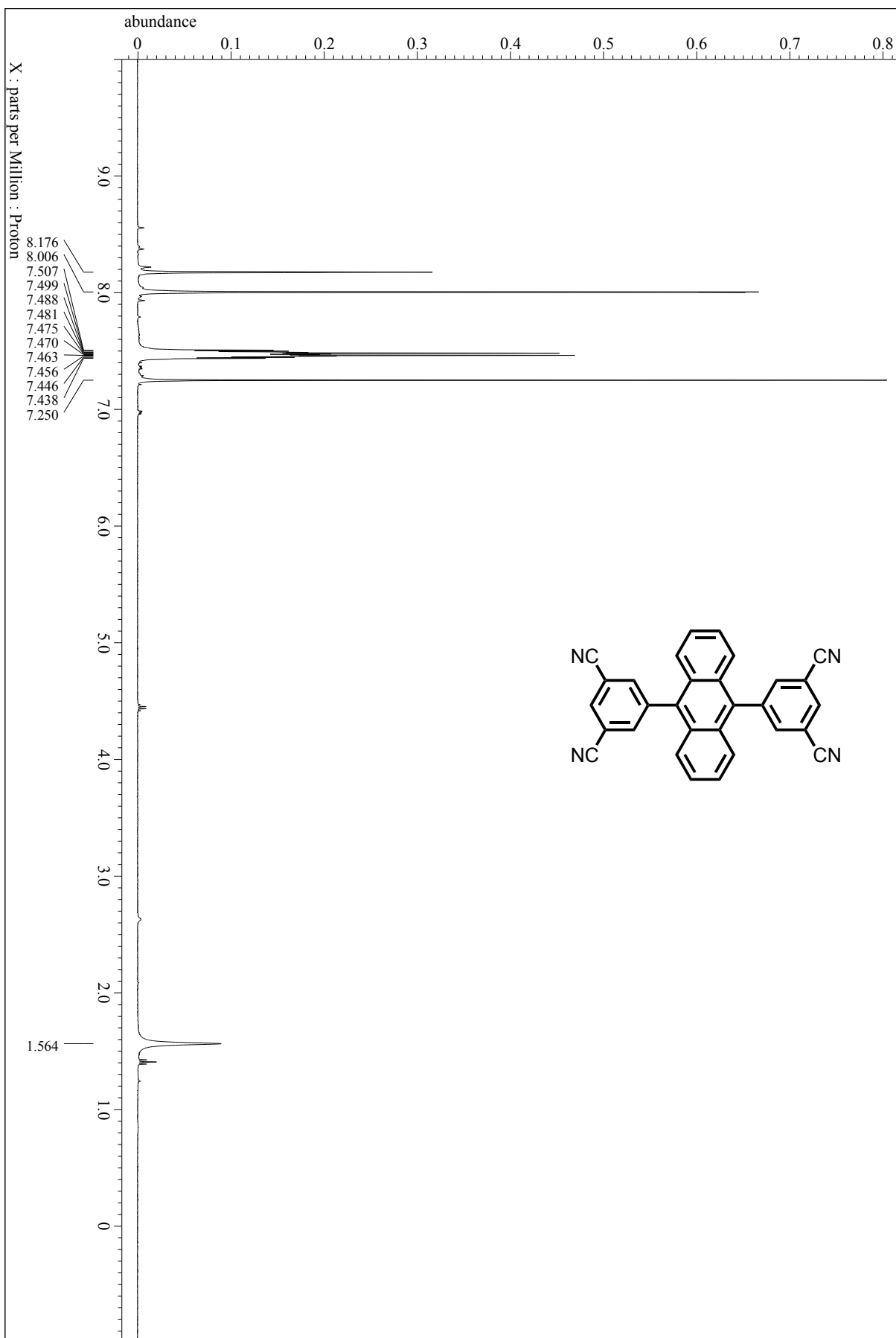
nitrogen passed through the mixture for 1 h. Then, tris(dibenzylideneacetone)dipalladium(0) (0.106 g, 0.116 mmol) and 2-dicyclohexylphosphino-2',6'-dimethoxybiphenyl (0.100 g, 0.243 mmol) were added and the resulting mixture was vigorously stirred for 24 hours at 75 ˚C under nitrogen. The resulting mixture was cooled to room temperature. Then, water was added to the mixture, and the organic layer was extracted with toluene, washed with water. The organic layer was separated, dried over anhydrous $MgSO_4$, and evaporated. The small amount of solution was purified by silica gel flash chromatography (Dichloromethane/hexane = 7:3 v/v) to afford DCA as a light-yellow solid (0.342 g, 34%): ^{1}H-NMR (400 MHz, $CDCl_3$): δ 8.17 (s, 2H), 8.00 (s, 4H), 7.52–7.41 (m, 8H) ppm. ^{13}C-NMR (100 MHz, $CDCl_3$): δ 141.9, 138.6, 134.8, 133.2, 129.5, 127.1, 125.8, 116.5, 114.8. MS (MALDI-TOF, *m/z*): Calcd for $C_{30}H_{14}N_4$:430.12; found: 429.80. Elemntal Anal.: Calcd for $C_{30}H_{14}N_4$: C 83.71, H 3.28, N 13.02; found: C 83.86, H 3.42, N 12.78.

abundance

X : parts per Million : Proton

7.773
7.764
7.755
7.747
7.352
7.344
7.335
7.327
7.250
6.638
3.832
1.552

$^1$H-NMR spectrum of DMA (400 MHz, CDCl$_3$)

S 5

$^{13}$C-NMR spectrum of DMA (100 MHz, CDCl$_3$)

$^1$H-NMR spectrum of DCA (400 MHz, CDCl$_3$)

X : parts per Million : Carbon13

(thousandths)

190.0 180.0 170.0 160.0 150.0 140.0 130.0 120.0 110.0 100.0 90.0 80.0 70.0 60.0 50.0 40.0 30.0 20.0 10.0 0

141.800
138.498
134.688
133.153
129.400
126.982
125.725
116.396
114.870
77.317
77.000
76.683
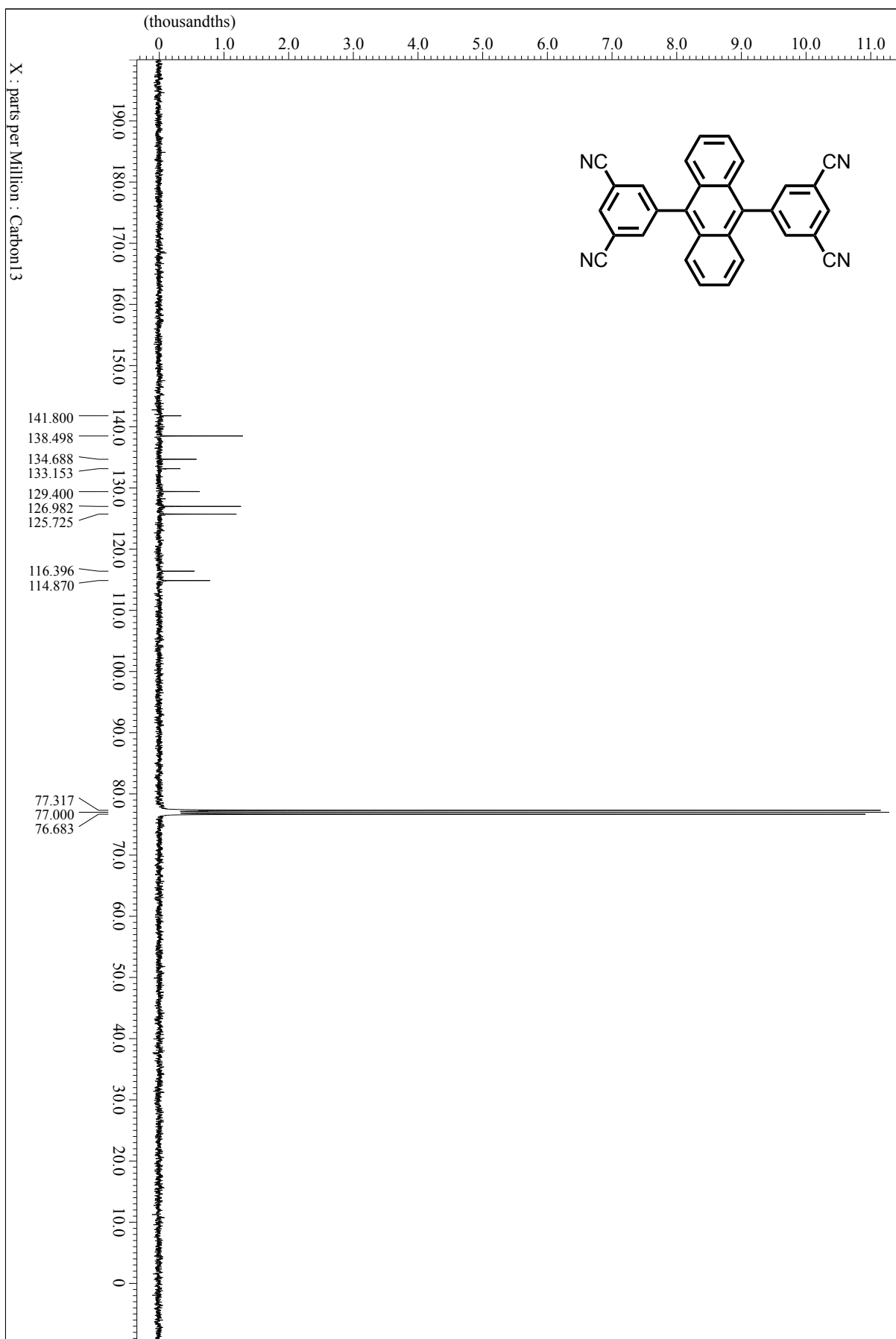
$^{13}$C-NMR spectrum of DCA (100 MHz, CDCl$_3$)

S 8

**Table S1** PL quantum yields ($\eta_{PL}$) for neat film: TAPC, DMA, DCA, CBP, and co-evaporated mixed films: TAPC:DMA, DMA:DCA, TAPC:DCA, TAPC:CBP, CBP:DCA.

| emitter | $\eta_{PL}$ (%) | emitter | $\eta_{PL}$ (%) |
|---------|------|----------|------|
| TAPC | 5.1 | TAPC:DMA | 9.8 |
| DMA | 14 | DMA:DCA | 39 |
| DCA | 35 | TAPC:DCA | 0.5 |
| CBP | 27 | TAPC:CBP | 9.3 |
| | | CBP:DCA | 42 |

**Table S2** Transient PL properties for neat films of TAPC, DMA, and DCA at 297 K in vacuum, detected at each emission peak.

| sample | $\tau_1$ (ns) | $A_1$ | $\Phi_1$ (%) | $\tau_2$ (ns) | $A_2$ | $\Phi_2$ (%) | $\langle\tau_{1,2}\rangle$ (ns) |
|--------|--------|--------|--------|--------|--------|--------|--------|
| TAPC | 0.10 | 0.514 | 74.5 | 1.27 | 0.0142 | 25.5 | 0.40 |
| DMA | 0.66 | 0.0898 | 87.4 | 3.23 | 0.00263 | 12.6 | 0.98 |
| DCA | 0.92 | 0.835 | 89.4 | 5.64 | 0.00161 | 10.6 | 0.98 |

**Table S3** Transient PL properties for co-evaporated mixed films of TAPC:DMA, DMA:DCA, and TAPC:DCA at 297 K in vacuum, detected at each emission peak.

| sample | $\tau_1$ (ns) | $A_1$ | $\Phi_1$ (%) | $\tau_2$ (ns) | $A_2$ | $\Phi_2$ (%) | $\tau_3$ (ns) | $A_3$ | $\Phi_3$ (%) |
|--------|--------|--------|--------|--------|--------|--------|--------|--------|--------|
| TAPC:DMA | 1.40 | 2.29 | 8.4 | 88.9 | 0.110 | 25.7 | 284 | 0.0884 | 65.9 |
| DMA:DCA | 4.55 | 0.796 | 20.3 | 32.3 | 0.294 | 53.1 | 125 | 0.0382 | 26.7 |
| TAPC:DCA | 2.25 | 1.17 | 4.1 | 95.2 | 0.226 | 33.7 | 299 | 0.133 | 62.2 |

**Table S4** Maximum external quantum efficiency ($\eta_{ext}$) of the exciplex OLEDs using the spacer.

| spacer | spacer distance (nm) | $\eta_{ext}$ (%) | luminance (cd/m²) | current density (mA/cm²) | voltage (V) |
|---|---|---|---|---|---|
| DMA | 0 | 0.14 | 388 | 104 | 6.6 |
| DMA | 10 | 0.43 | 293 | 30.7 | 5.2 |
| DMA | 20 | 0.37 | 24 | 3.3 | 4.2 |
| DMA | 30 | 0.33 | 65 | 8.5 | 5.2 |
| DMA | 40 | 0.42 | 716 | 94.4 | 8.4 |
| DMA | 50 | 0.48 | 360 | 41.0 | 7.8 |
| DMA | 60 | 0.69 | 361 | 37.9 | 8.2 |
| DMA | 70 | 0.86 | 418 | 40.0 | 8.8 |
| CBP | 0 | 0.14 | 388 | 104 | 6.6 |
| CBP | 1 | 0.33 | 659 | 89.1 | 6.6 |
| CBP | 5 | 0.55 | 589 | 45.9 | 5.6 |
| CBP | 10 | 0.72 | 389 | 22.8 | 5.2 |
| CBP | 15 | 1.6 | 724 | 38.4 | 6.6 |
| CBP | 20 | 3.0 | 16.8 | 0.59 | 4.0 |

**Table S5** Temperature dependence of the transient PL properties for neat film of DMA in vacuum, detected at the emission peak.

| temp. (K) | $\tau_1$ (ns) | $A_1$ | $\Phi_1$ (%) | $\tau_2$ (ns) | $A_2$ | $\Phi_2$ (%) | $\tau_3$ (ns) | $A_3$ | $\Phi_3$ (%) |
|---|---|---|---|---|---|---|---|---|---|
| 297 | 0.845 | 0.199 | 47.6 | 1.74 | 0.103 | 50.5 | 9.54 | 0.000719 | 1.9 |
| 257 | 1.01 | 0.213 | 54.4 | 2.54 | 0.0650 | 41.9 | 12.6 | 0.00116 | 3.7 |
| 207 | 1.50 | 0.186 | 53.6 | 5.80 | 0.0303 | 33.9 | 20.1 | 0.00323 | 12.5 |
| 157 | 1.72 | 0.143 | 29.7 | 8.99 | 0.0386 | 41.9 | 31.8 | 0.00739 | 28.4 |
| 107 | 1.88 | 0.111 | 17.4 | 11.0 | 0.0493 | 45.5 | 33.6 | 0.0132 | 37.2 |
| 77 | 2.20 | 0.0917 | 16.6 | 11.0 | 0.0522 | 47.1 | 32.7 | 0.0135 | 36.3 |

**Table S6** Temperature dependence of the transient PL properties for a co-evaporated mixed film of TAPC:DCA in vacuum, detected at the emission peak.

| temp. (K) | $\tau_1$ (ns) | $A_1$ | $\Phi_1$ (%) | $\tau_2$ (ns) | $A_2$ | $\Phi_2$ (%) | $\tau_3$ (ns) | $A_3$ | $\Phi_3$ (%) |
|---|---|---|---|---|---|---|---|---|---|
| 297 | 1.62 | 2.18 | 8.4 | 104 | 0.127 | 31.5 | 317 | 0.0799 | 60.2 |
| 257 | 1.66 | 2.25 | 8.6 | 127 | 0.0957 | 28.1 | 383 | 0.0714 | 63.3 |
| 207 | 1.88 | 1.78 | 6.6 | 155 | 0.101 | 30.8 | 467 | 0.0685 | 62.6 |
| 157 | 1.78 | 1.98 | 6.6 | 155 | 0.0928 | 27.0 | 518 | 0.0681 | 66.4 |
| 107 | 1.96 | 1.78 | 7.2 | 146 | 0.0823 | 24.8 | 547 | 0.0602 | 68.0 |
| 77 | 1.93 | 1.79 | 6.5 | 156 | 0.0831 | 24.3 | 592 | 0.0622 | 69.2 |

**Table S7** Temperature dependence of the transient PL properties for a stacked film of TAPC (2 nm)/DMA (10 nm)/DCA (2 nm) in vacuum, detected at 550 nm for the exciplex emission of TAPC and DCA.

| temp. (K) | $\tau_1$ (ns) | $A_1$ | $\Phi_1$ (%) | $\tau_2$ (ns) | $A_2$ | $\Phi_2$ (%) | $\tau_3$ (ns) | $A_3$ | $\Phi_3$ (%) |
|---|---|---|---|---|---|---|---|---|---|
| 297 | 0.949 | 0.589 | 22.5 | 12.1 | 0.0323 | 15.8 | 152 | 0.0100 | 61.7 |
| 257 | 0.830 | 0.676 | 21.8 | 10.6 | 0.0332 | 13.7 | 170 | 0.00976 | 64.5 |
| 207 | 1.30 | 0.459 | 18.1 | 24.2 | 0.0203 | 14.9 | 194 | 0.0114 | 67.0 |
| 157 | 1.40 | 0.434 | 15.0 | 25.9 | 0.0301 | 19.2 | 209 | 0.0128 | 65.9 |
| 107 | 1.28 | 0.436 | 14.5 | 20.2 | 0.0314 | 16.6 | 198 | 0.0133 | 68.9 |
| 77 | 1.36 | 0.420 | 14.6 | 20.7 | 0.0319 | 17.0 | 202 | 0.0132 | 68.5 |

**Table S8** Transient PL properties for stacked film of TAPC (2 nm)/DMA (x nm)/DCA (2 nm) in vacuum.

| distance (nm) | $\lambda_{em}$ (nm) | $\tau_1$ (ns) | $A_1$ | $\Phi_1$ (%) | $\tau_2$ (ns) | $A_2$ | $\Phi_2$ (%) | $\tau_3$ (ns) | $A_3$ | $\Phi_3$ (%) |
|---|---|---|---|---|---|---|---|---|---|---|
| 0 | 550 | 1.32 | 1.15 | 28.0 | 17.9 | 0.0490 | 16.2 | 160 | 0.0190 | 55.8 |
| 10 | 550 | 0.986 | 0.573 | 22.3 | 13.2 | 0.0305 | 15.9 | 160 | 0.00974 | 61.8 |
| 20 | 550 | 2.83 | 1.30 | 21.0 | 42.9 | 0.114 | 27.8 | 253 | 0.0355 | 51.3 |
| 30 | 550 | 5.23 | 0.910 | 23.0 | 62.4 | 0.108 | 32.5 | 292 | 0.0316 | 44.6 |
| 50 | 550 | 3.58 | 1.09 | 23.5 | 42.1 | 0.116 | 29.5 | 242 | 0.0320 | 46.9 |
| 70 | 550 | 2.34 | 1.37 | 31.5 | 28.0 | 0.0942 | 25.8 | 232 | 0.0188 | 42.7 |
| 10 | 440 | 0.839 | 0.689 | 73.1 | 5.46 | 0.0216 | 18.1 | 33.8 | 0.00206 | 8.8 |

**Table S9** Transient PL properties for stacked film of TAPC (2 nm)/CBP (x nm)/DCA (2 nm) in vacuum.

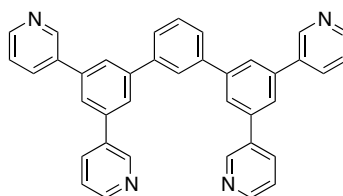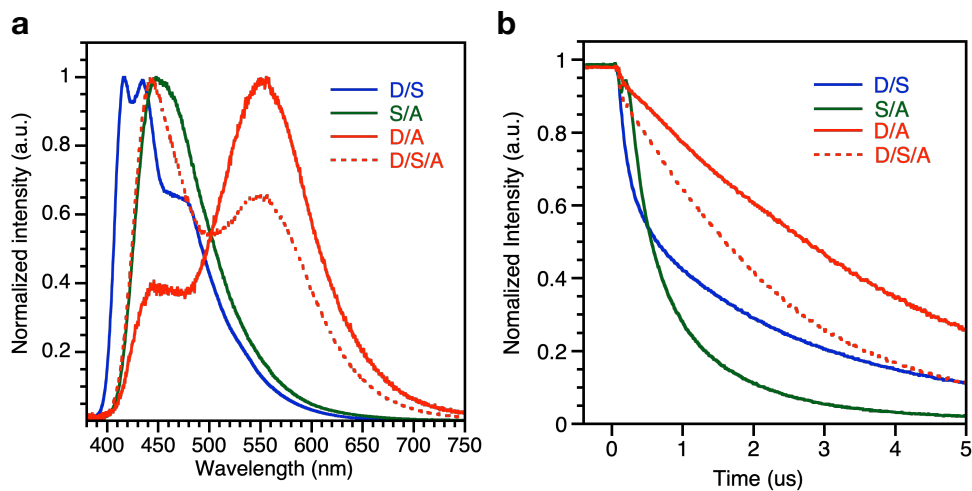| distance (nm) | $\lambda_{em}$ (nm) | $\tau_1$ (ns) | $A_1$ | $\Phi_1$ (%) | $\tau_2$ (ns) | $A_2$ | $\Phi_2$ (%) | $\tau_3$ (ns) | $A_3$ | $\Phi_3$ (%) |
|---|---|---|---|---|---|---|---|---|---|---|
| 0 | 550 | 1.32 | 1.15 | 28.0 | 17.9 | 0.0490 | 16.2 | 160 | 0.0190 | 55.8 |
| 5 | 550 | 1.33 | 0.419 | 20.0 | 18.0 | 0.0277 | 17.8 | 162 | 0.0107 | 62.1 |
| 10 | 550 | 1.40 | 0.392 | 24.5 | 13.1 | 0.0415 | 24.3 | 145 | 0.00788 | 51.2 |
| 15 | 550 | 2.00 | 0.308 | 33.6 | 12.9 | 0.0517 | 36.3 | 111 | 0.00497 | 30.2 |
| 20 | 550 | 1.81 | 0.318 | 32.4 | 11.3 | 0.0636 | 40.5 | 84.9 | 0.00567 | 27.1 |
| 10 | 400 | 0.118 | 27.3 | 94.9 | 3.05 | 0.0328 | 3.0 | 16.1 | 0.00456 | 2.2 |

**Fig. S1** Chemical structure of B3PyPB.



**Fig. S2** a) EL spectra of the devices at 25 mA/cm². b) Transient EL decay at 50 mA/cm². The applied voltages are 7.19 V for D/S device, 5.50 V for S/A device, 5.97 V for D/A device, and 6.89 V for D/S/A device. The device configurations are the followings:

D/S: ITO/ PEDOT:PSS (30 nm)/ TAPC (20 nm)/ DMA (30 nm)/ B3PyPB (40 nm)/ LiF (1 nm)/ Al

S/A: ITO/ MoO$_3$ (5 nm)/ DMA (30 nm)/ DCA (10 nm)/ B3PyPB (40 nm)/ LiF (1 nm)/ Al

D/A: ITO/ PEDOT:PSS (30 nm)/ TAPC (20 nm)/ DCA (10 nm)/ B3PyPB (40 nm)/ LiF (1 nm)/ Al

D/S/A: ITO/ PEDOT:PSS (30 nm)/ TAPC (20 nm)/ DMA (30 nm)/ DCA (10 nm)/ B3PyPB (40 nm)/ LiF (1 nm)/ Al

a
Ra 0.37 nm

b
Ra 0.33 nm

c
Ra 0.84 nm

| TAPC (20 nm) |
| PEDOT:PSS (30 nm) |
| ITO |

| DMA (30 nm) |
| TAPC (20 nm) |
| PEDOT:PSS (30 nm) |
| ITO |

| DCA (10 nm) |
| DMA (30 nm) |
| TAPC (20 nm) |
| PEDOT:PSS (30 nm) |
| ITO |
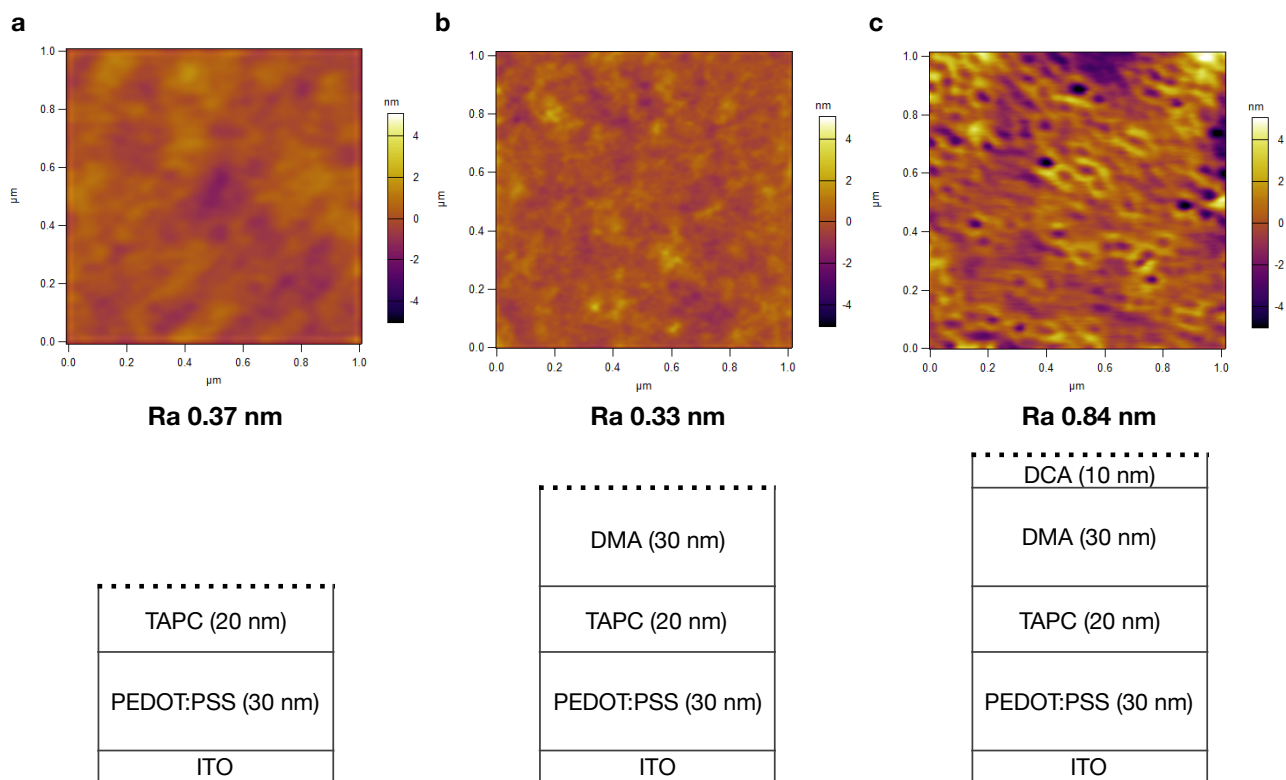
**Fig. S3** AFM images and schematic film configurations of a) ITO/PEDOT: PSS (30 nm)/TAPC (20 nm), b) ITO/PEDOT: PSS (30 nm)/TAPC (20 nm)/DMA (30 nm), and c) ITO/PEDOT: PSS (30 nm)/TAPC (20 nm)/DMA (30 nm)/DCA (10 nm). The dashed lines in the schematics are the measured surfaces.
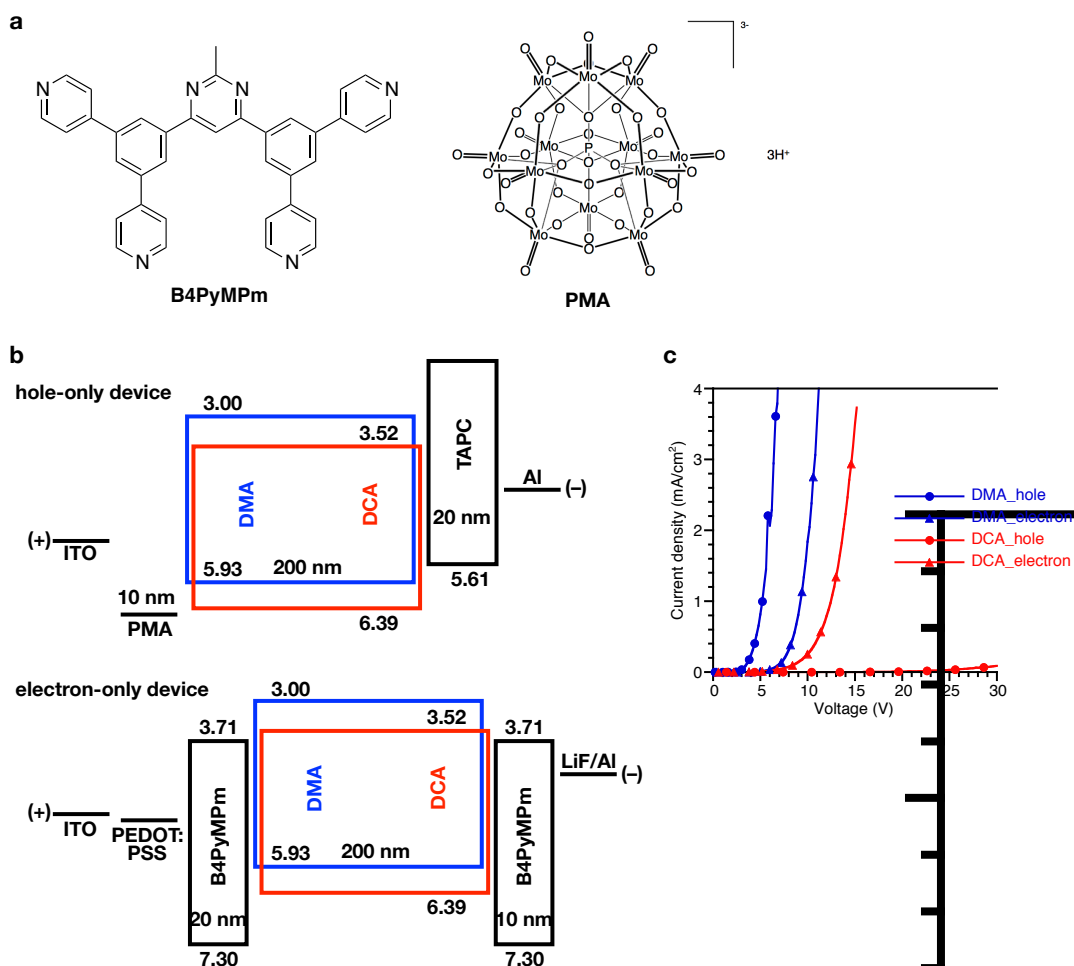
**Fig. S4** Hole- and electron-only devices for DMA and DCA. a) Chemical structure of B4PyMPm and PMA. b) Device structures. c) Current density-voltage plots of the devices.
Hole-only device: ITO/ PMA (10 nm)/ DMA or DCA (200 nm)/ TAPC (20 nm)/ Al (80 nm)
Electron-only device: ITO/ PEDOT:PSS (30 nm)/ B4PyMPM (20 nm)/ DMA or DCA (200 nm)/ B4PyMPM (10 nm)/ LiF (1 nm)/ Al (80 nm)
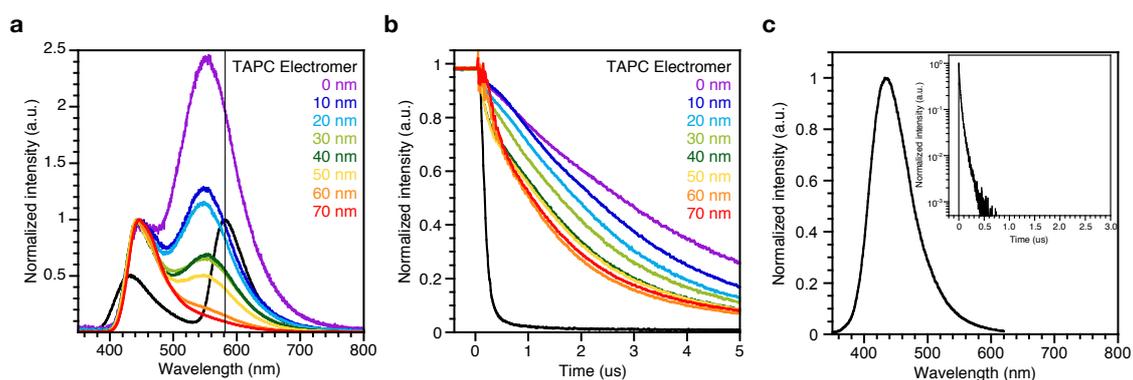


**Fig. S5** TAPC electromer. a) EL spectra at 25 mA/cm$^2$, superimposed on Fig. 2b for comparison. b) Transient EL decay at 50 mA/cm$^2$, superimposed on Fig. 2c. c) PL spectrum of the co-evaporated film TAPC:B3PyPB ($\lambda_{ex}$ 330 nm) and the transient PL decay ($\lambda_{ex}$ 280 nm, $\lambda_{em}$ 435 nm). The device structure: ITO/ PEDOT:PSS (30 nm)/ TAPC (15 nm)/ B3PyPB (60 nm)/ LiF (1 nm)/ Al (80 nm).
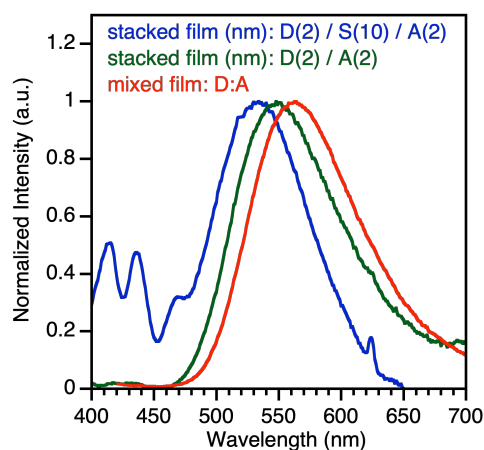
**Fig. S6** Energy shift of the exciplex emission in the PL spectra ($\lambda_{ex}$ 380 nm for D/S/A film and $\lambda_{ex}$ 400 nm for D/A and D:A films).
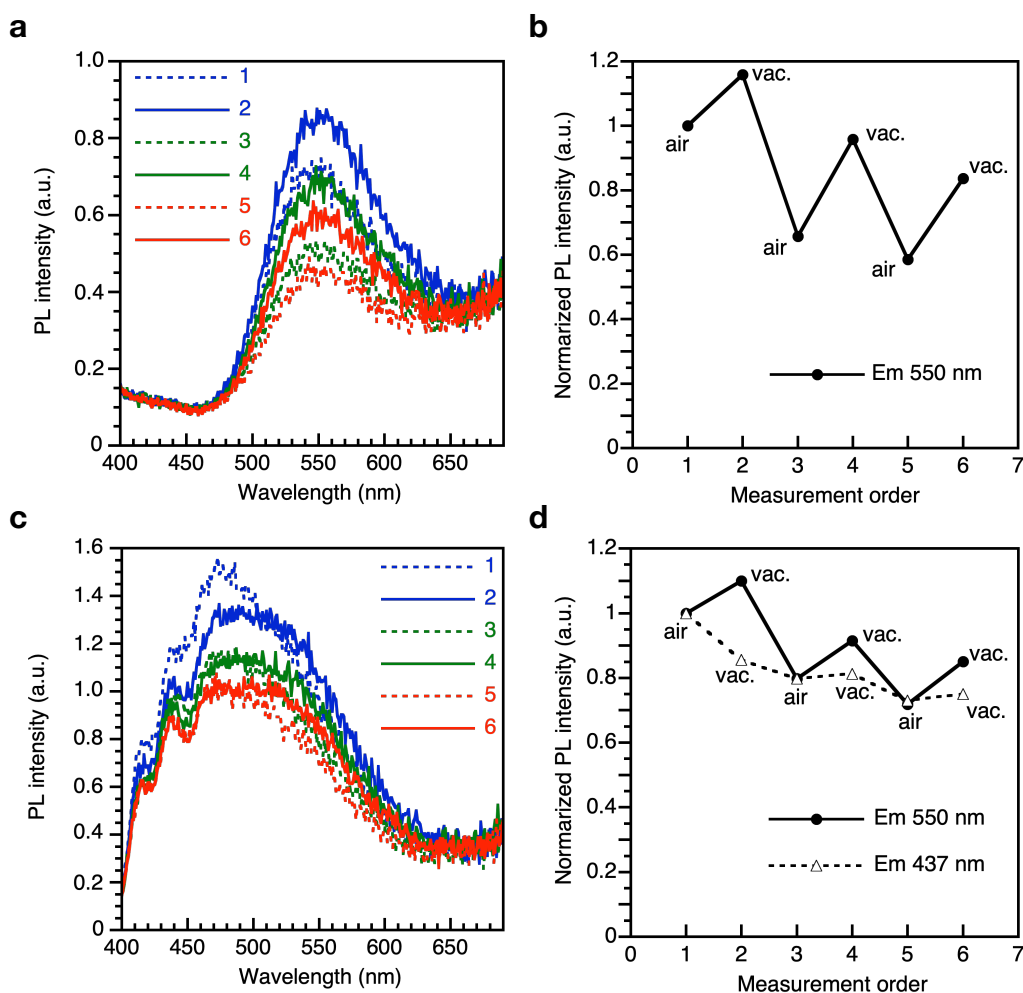


**Fig. S7** a) PL spectra of TAPC (2 nm)/ DCA(2 nm) layers ($\lambda_{ex}$ 380 nm) in air (dashed line) and vacuum (solid line). The numbers indicate the measurement order. b) PL intensities of TAPC (2 nm)/ DCA(2 nm) layers ($\lambda_{ex}$ 380 nm) at 550 nm as a function of the measurement order. c) PL spectra of TAPC (2 nm)/ DMA (10 nm)/ DCA(2 nm) layers ($\lambda_{ex}$ 380 nm) in air (dashed line) and vacuum (solid line). The numbers indicate the measurement order. d) PL intensities of TAPC (2 nm)/ DMA (10 nm)/ DCA(2 nm) layers ($\lambda_{ex}$ 380 nm) at 550 nm (solid circle) and 437 nm (open triangle) as a function of the measurement order.
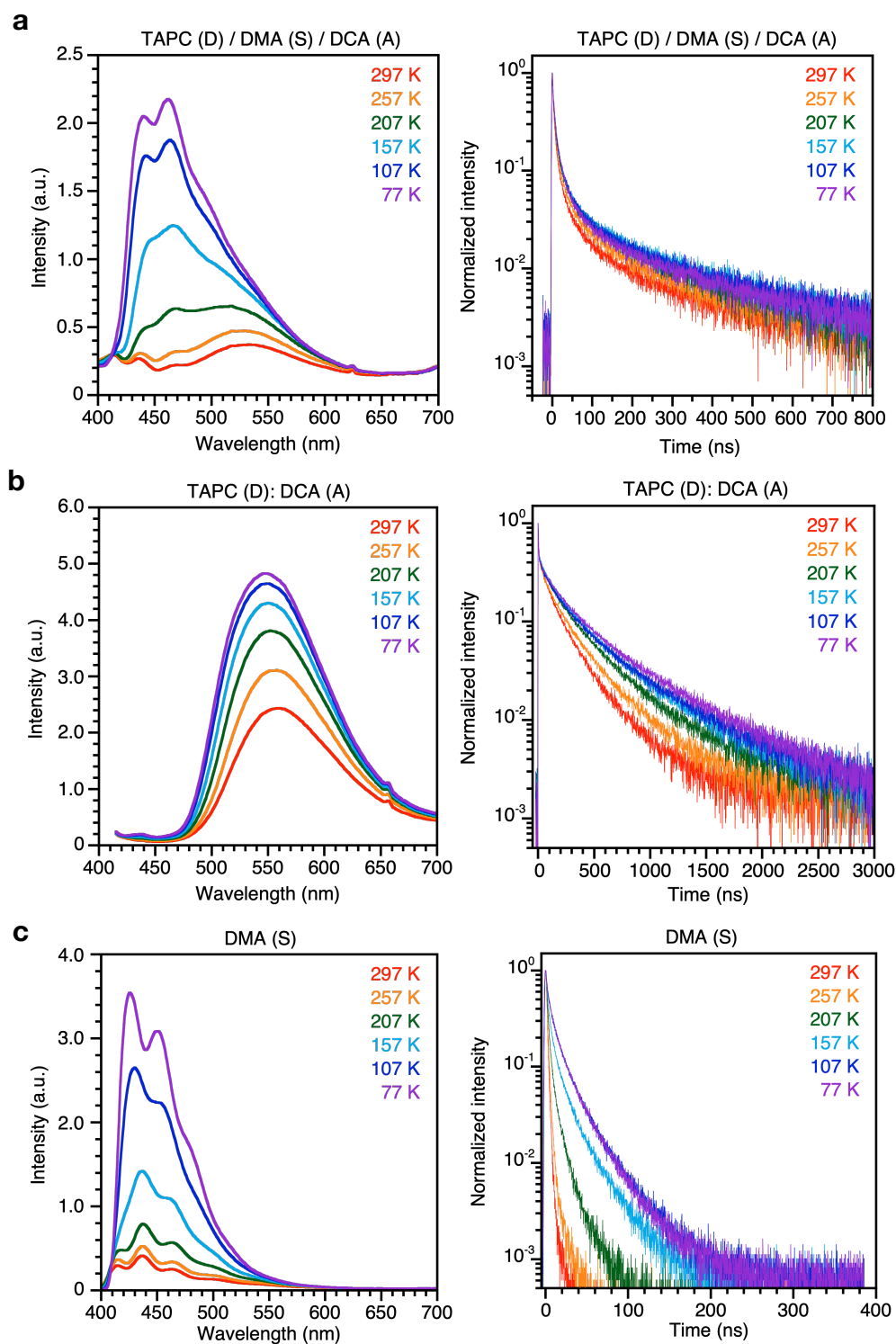
**Fig. S8** Temperature dependence of the PL spectra and transient PL decay. a) TAPC (2 nm)/DMA (10 nm)/ DCA (2 nm) ($\lambda_{ex}$ 380 nm for PL; $\lambda_{ex}$ 370 nm and $\lambda_{em}$ 550 nm for transient PL). b) TAPC: DCA (20 nm) ($\lambda_{ex}$ 400 nm for PL; $\lambda_{ex}$ 370 nm and $\lambda_{em}$ 550 nm for transient PL). c) DMA (20 nm) ($\lambda_{ex}$ 360 nm for PL; $\lambda_{ex}$ 370 nm and $\lambda_{em}$ 440 nm for transient PL).
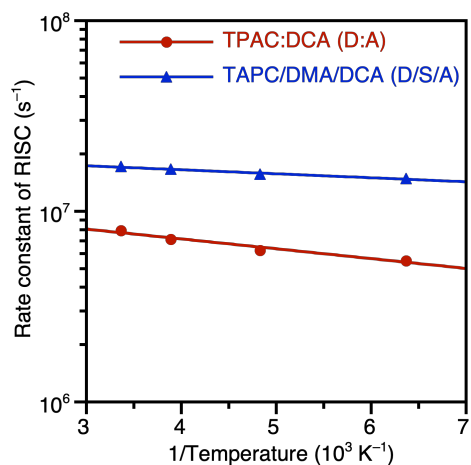
**Fig. S9** Arrhenius plots of the rate constants of reverse intersystem crossing ($k_{RISC}$) for a mixed TAPC:DCA film (20 nm) and a stacked TAPC (2 nm)/ DMA (10 nm)/ DCA (2 nm) film. The solid lines represent single exponential fits according to the Arrhenius model $k_{RISC} = A \exp(-E_a/k_B T)$, where $A$ is a constant, $E_a$ is the energy difference between the lowest-excited singlet and triplet states, $k_B$ is the Boltzmann constant, and $T$ is the temperature.
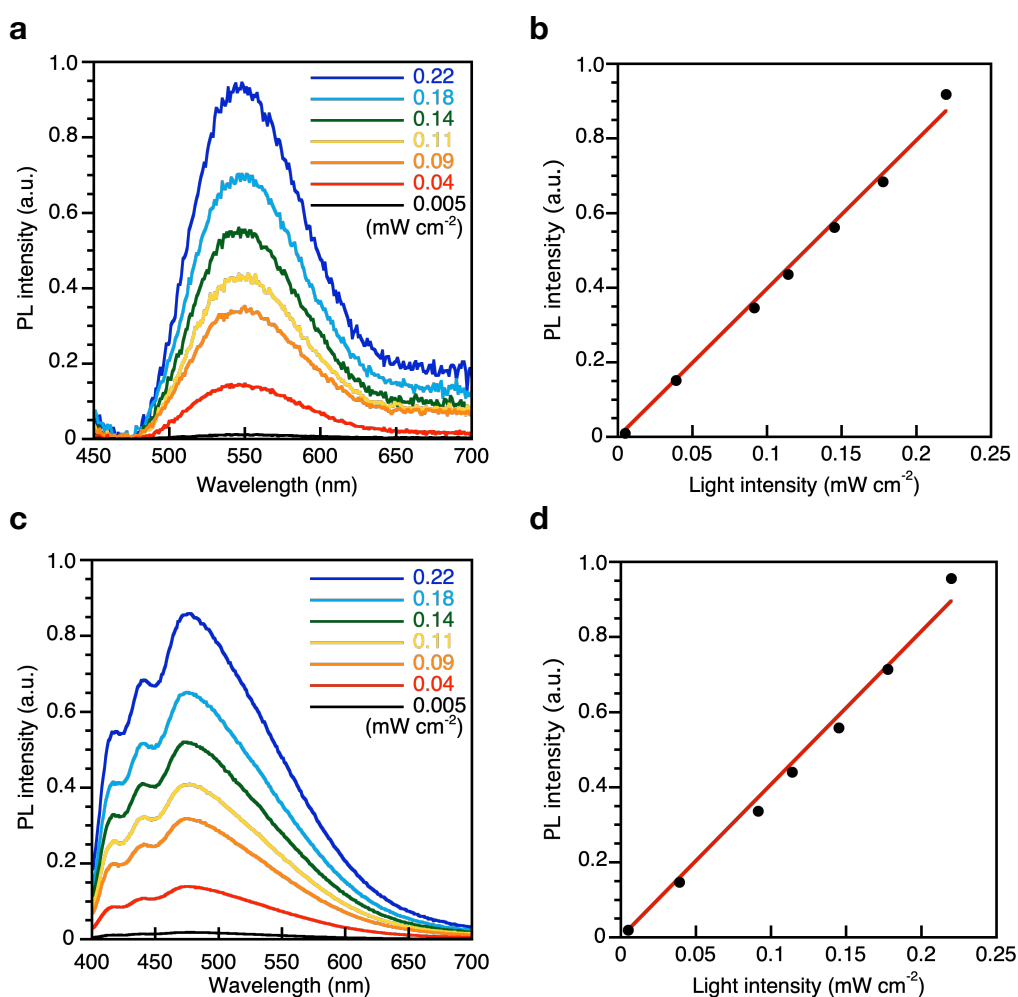


**Fig. S10** Excitation light intensity dependence of a) the PL spectra of TAPC (2 nm) / DCA(2 nm) layers ($\lambda_{ex}$ 380 nm), b) the PL intensity at 550 nm, c) the PL spectra of TAPC (2 nm) / DMA (10 nm) / DCA(2 nm) layers ($\lambda_{ex}$ 380 nm), and d) the PL intensity at 550 nm.
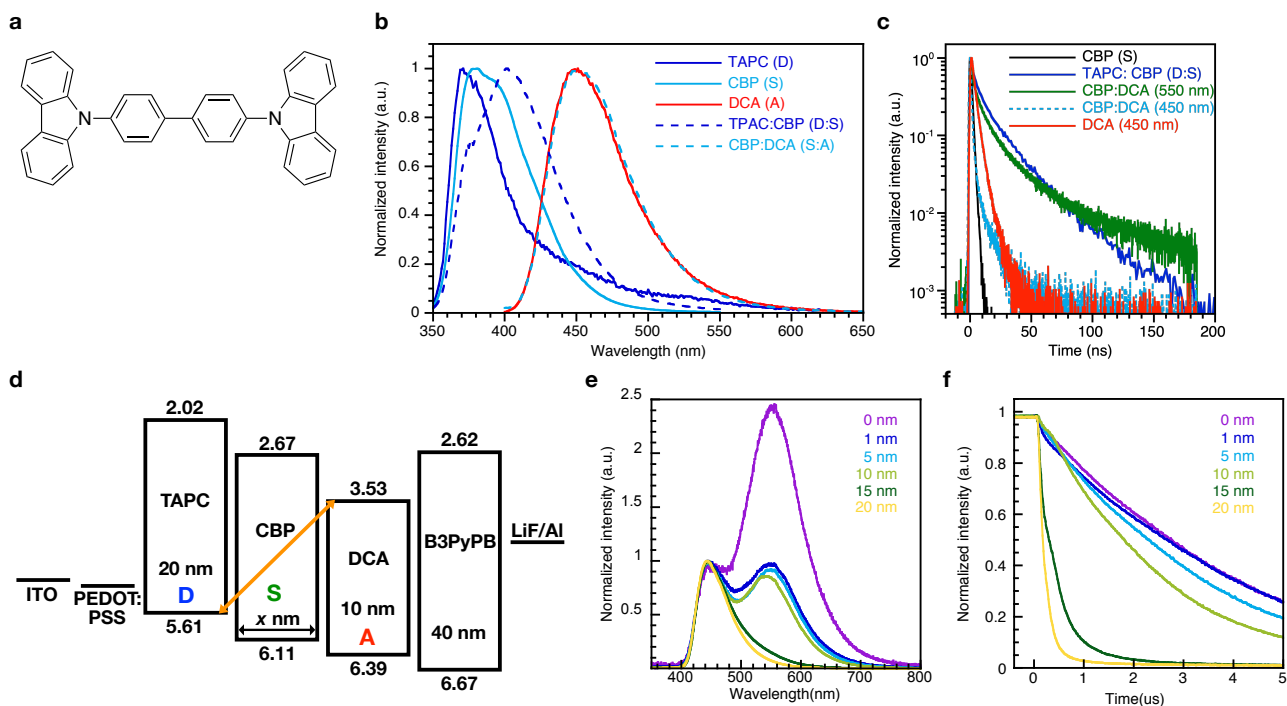
**Fig. S11** Spacer distance dependent EL in the device with CBP spacer. a) Chemical structure of CBP. b) PL spectra of the neat films and the co-evaporated (1/1 wt/wt) films. CBP ($\lambda_{ex}$ 300 nm), TAPC:CBP ($\lambda_{ex}$ 300 nm), CBP:DCA ($\lambda_{ex}$ 380 nm). c) Transient PL decay of the neat films and the co-evaporated (1/1 wt/wt) films: TAPC ($\lambda_{ex}$ 280 nm, $\lambda_{em}$ 375 nm), CBP ($\lambda_{ex}$ 290 nm, $\lambda_{em}$ 380 nm), DCA ($\lambda_{ex}$ 365 nm, $\lambda_{em}$ 450 nm), TAPC:CBP ($\lambda_{ex}$ 340 nm, $\lambda_{em}$ 400 nm), CBP:DCA ($\lambda_{ex}$ 365 nm, $\lambda_{em}$ 550 nm or 450 nm). d) Device structure. e) EL at 25 mA/cm$^2$ with different spacer thicknesses. f) Transient EL decay at 50 mA/cm$^2$ with different spacer thicknesses. The applied voltages are 5.50 V for 0 nm, 5.68 V for 1 nm, 5.72 V for 5 nm, 6.11 V for 10 nm, 6.97 V for 15 nm, and 7.00 V for 20 nm.
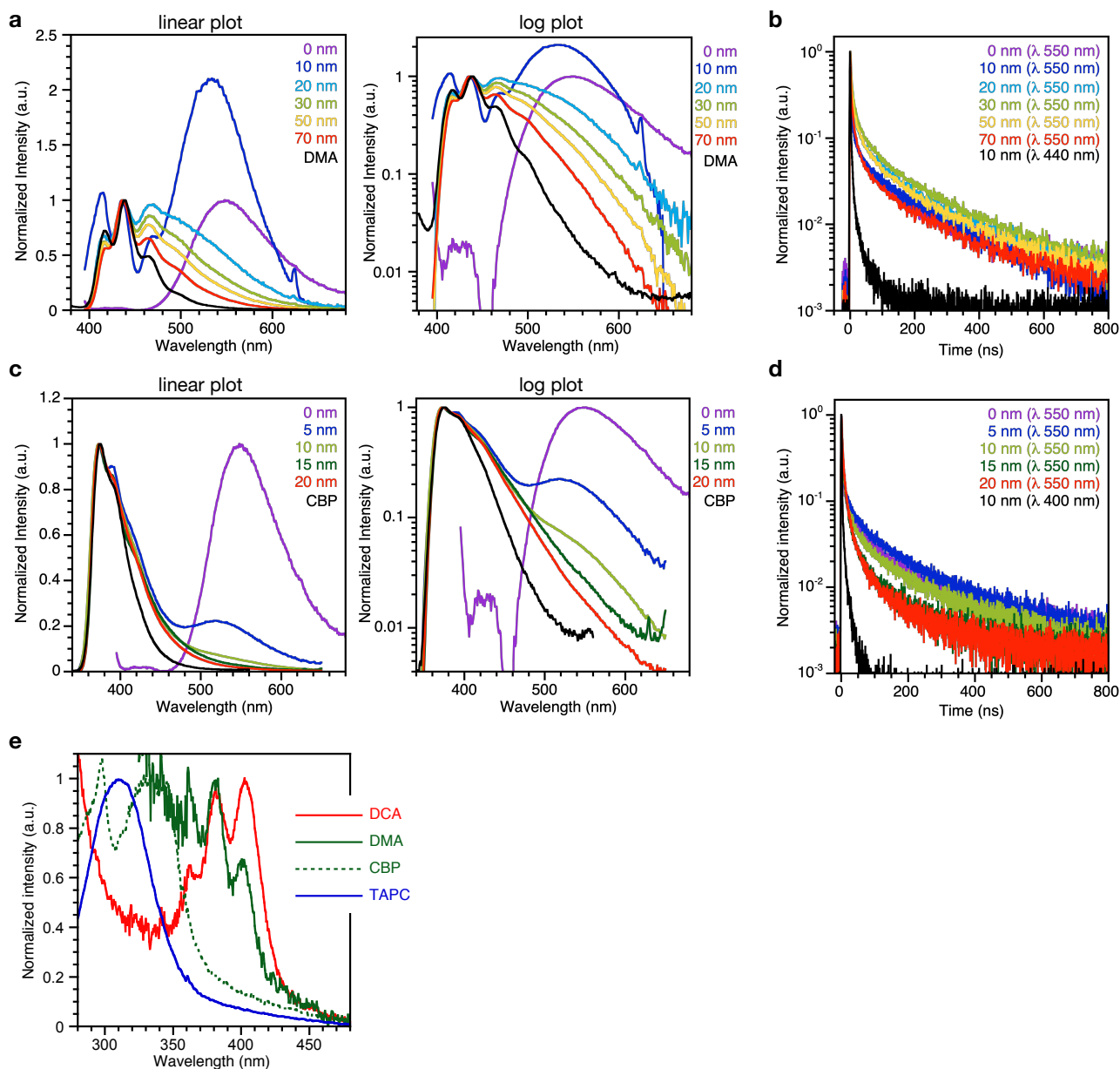
S18

**Fig. S12** Spacer distance dependence of the stacked film PL. Excitation light was incident from the side of DCA layer. a) PL spectra of quartz/ TAPC (2 nm)/ DMA (*x* nm)/ DCA (2 nm) ($\lambda_{ex}$ 380 nm) and neat film of DMA ($\lambda_{ex}$ 360 nm). b) Transient PL decay with DMA spacer ($\lambda_{ex}$ 370 nm and $\lambda_{em}$ 550 nm for the spacer thickness from 0 nm to 70 nm; $\lambda_{ex}$ 370 nm and $\lambda_{em}$ 440 nm for the 10 nm spacer thickness). c) PL spectra of quartz/ TAPC (2 nm)/ CBP (*x* nm)/ DCA (2 nm) ($\lambda_{ex}$ 330 nm) and neat film of CBP ($\lambda_{ex}$ 290 nm). d) Transient PL decay with CBP spacer ($\lambda_{ex}$ 370 nm and $\lambda_{em}$ 550 nm for the spacer thickness from 0 nm to 20 nm; $\lambda_{ex}$ 370 nm and $\lambda_{em}$ 400 nm for the 10 nm spacer thickness). e) UV-vis absorption spectra of neat film of DCA, DMA, CBP, and TAPC.
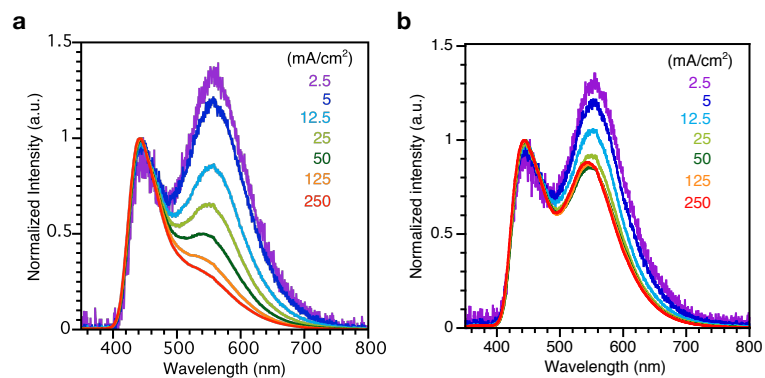
S19

**Fig. S13** Current density and voltage dependence of EL spectra. a) Device with 30 nm DMA spacer. The applied voltages are 4.33 V for 2.5 mA/cm$^2$, 4.78 V for 5 mA/cm$^2$, 5.55 V for 12.5 mA/cm$^2$, 6.21 V for 25 mA/cm$^2$, 6.90 V for 50 mA/cm$^2$, 7.94 V for 125 mA/cm$^2$, and 8.87 V for 250 mA/cm$^2$. b) Device with 5 nm CBP spacer. The applied voltages are 3.63 V for 2.5 mA/cm$^2$, 3.87 V for 5 mA/cm$^2$, 4.35 V for 12.5 mA/cm$^2$, 4.89 V for 25 mA/cm$^2$, 5.72 V for 50 mA/cm$^2$, 7.26 V for 125 mA/cm$^2$, and 8.96 V for 250 mA/cm$^2$.